17th World Conference on Earthquake Engineering, 17WCEE
Sendai, Japan - September 13th to 18th 2020

DYNAMIC ANALYSIS OF SELF-CENTERING CONCENTRICALLY BRACED FRAMES WITHIN THE MIXED LAGRANGIAN FORMULATION

A. Marzok [1], O. Lavan [2]

[1] *Ph.D. candidate, Faculty of Civil and Environmental Engineering, Technion – Israel Institute of Technology, Technion City, Haifa, Israel, ameerm@campus.technion.ac.il*

[2] *Associate professor, Faculty of Civil and Environmental Engineering, Technion – Israel Institute of Technology, Technion City, Haifa, Israel, lavan@technion.ac.il*

Abstract

In the last years, with the development of performance based seismic design, extensive research on damage free systems such as self-centering has been conducted. The ability of these systems to eliminate residual drifts was found to be beneficial from an economic point of view. This is due to the reduced amount of damage and repair costs with the end of the seismic event. Self-Centering Concentrically Braced Frames (SC-CBF) showed high performance in previous experimental studies. They survived experimental ground shakes with reduced damage to the primary structural elements while eliminating residual drifts. Generally, column uplift is allowed at the base of SC-CBFs and Post-Tensioned (PT) tendon is provided to create a flexural moment in the opposite direction to the overturning moment. This leads to a reduction in the residual displacements. The behavior of the system is nonlinear elastic while the energy dissipation (ED) is achieved by different types of dampers provided at the rocking sections (e.g. metallic yield dampers or viscous dampers).

Higher vibration mode effects may lead to large shear force and flexural moment demands through the building height. Following the capacity design philosophy, these high demands could lead to the design of large structural members and an increase in the building cost. Adding rocking sections at higher levels, where the flexural moments from the higher vibration modes are expected to be large, could reduce significantly the design force demands. To date, rocking systems have been modeled either by using a simplified nonlinear rotational spring-based element or by using displacement-based finite-element methods (FEM). Using the first approach, a spring-based element is formulated to describe the global flag-shaped behavior of the self-centering mechanism. While this approach is computationally efficient, it is not suitable for modeling multiple rocking sections. This is due to the coupling between the rocking sections and its substantial effect on the PT elongation. In addition, it cannot analyze rocking structures subjected to varying external axial loads. Using the second approach, modeling of zero length contact elements is required. Thus, in order to prevent instability issues of the analysis and to ensure convergence, small time step sizes may be needed. This may be attributed to the abrupt stiffness change at the time of contact and its dependence on the relative displacements between the rocking sections due to columns uplifts. While small time step sizes are generally required when rocking is analyzed, this is more pronounced when multiple rocking locations exist in the structure. In view of the above, more robust time integration schemes that can analyze systems with multiple rocking sections are needed.

To overcome this gap, a new model based on the Mixed Lagrangian Formulation (MLF) is proposed. MLF was originally developed for the analysis of skeletal structures including plastic and geometrically nonlinear behavior. Later a gap element was added to describe contact behavior. It has been shown in previous research that the MLF has many advantages for the solution of dynamic problems especially when contact is expected and causing an abrupt change in the contact force. Hamilton's principle is discretized in time to produce an optimization problem at each time step. This optimization problem has a quadratic form and its solution is straightforward with the available numerical tools. The formulation of new systems in MLF is not yet straightforward. In this study, a new model is developed for rocking structures with multiple rocking sections. Both the internal forces and the global displacements are essential state variables in the MLF, and momentum conservation is considered automatically. Therefore, the proposed model shows high convergence stability even with relatively large time steps.

Keywords: Mixed-Lagrangian-Formulation, Self-Centering, Higher Mode Effects, Multiple Rocking Systems, Rocking Walls

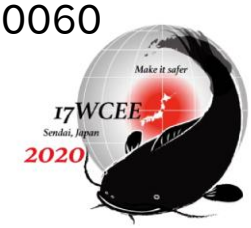

1. Introduction

Recent earthquakes have shown that buildings are exposed to large damage [1–3]. This damage causes high economic losses. These losses consist of direct and indirect losses. The former includes the damage to the building and its restoration costs. The latter includes business interruption and loss of the functionality of the building [4]. In addition, the restoration of these buildings is occasionally not feasible or even not possible. This is due to the existence of permanent residual deformations in the structural elements due to plastic behavior [5].

Damage free self-centering systems have shown experimentally negligible damage when subjected to seismic excitation [6,7]. Furthermore, their self-centering capability ensures that the residual deformations are negligible. Self-Centering-Concentrically Braced Frames (SC-CBFs) are an example of such systems [8]. In these systems, column uplift is permitted usually at the base of the building at the connection with the foundation. Post-tensioned cable is usually provided to ensure the self-centering behavior of such a system. Different solutions for Energy Dissipation (ED) are available and they can be designed at the rocking section or in other places of the structural system. This includes metallic yield bars or plates [9,10], fluid viscous dampers [6], shear fuses [11], etc. The hysteretic behavior of the rocking sections is usually referred to as flag shaped for the case of metallic yield dampers.

It has been shown that in traditional designs where the rocking behavior is concentrated at the base of the structural system, large flexural moment and shear force demands can develop through the height of the SC-CBF [12]. This phenomenon is attributed to the higher vibration modes effect. Therefore, additional rocking sections can be potentially added at higher levels of the SC-CBF. It has been shown that this solution can reduce significantly the shear force and flexural moment demands while preserving acceptable deformations [13]. This reduction is expected to lead to more economic designs [14].

Several analytical models were proposed for the analysis of rocking systems [15] and multiple rocking systems [12,13]. In general, these models have been developed based on the Finite Element Method (FEM). The rocking behavior includes contact between the two adjacent rocking sections. This behavior is modeled usually using contact gap elements. These elements include a nonlinear behavior that depends explicitly on the relative displacement between the surfaces of the rocking sections. An infinite stiffness is provided to the latter to describe the rigid contact in the compression phase. These elements have zero stiffness in tension which describes the vertical column uplifts.

Large numbers are often used to describe numerically the infinite stiffness. This may cause an ill-condition stiffness matrix. Therefore, the contact elements can be replaced by constraints on the displacements of the contact surface [16]. However, in both methods the behavior depends explicitly on the relative displacement between the contact surfaces. In rocking behavior, the duration of the contact can be very small. This leads to the need for small time-increments to ensure convergence.

Computationally efficient macro models have been proposed for systems with multiple rocking sections. In these models, rotational springs are added at the rocking surfaces with flag shaped hysteretic behavior [12]. The latter is calculated based on the properties of the rocking section prior to the analysis. Therefore, variable axial loads are not considered. In addition, the interaction between the different rocking sections is neglected in these models. This might cause unconservative estimations of the behavior in the case where the same cable is provided to more than one rocking section [13].

The existing models for SC-CBFs are usually based on FEM formulations. In the later, the behavior of the structural elements is related to the relative displacement. This might cause convergence issues when the duration of the contact is small such in SC-CBFs. Other models are more computationally efficient; however, they neglect the interaction between the rocking sections. Therefore, in this paper, a new model for the analysis of such systems is proposed.

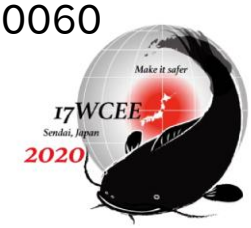

The proposed model is developed based on the Mixed-Lagrangian-Formulation (MLF). The main advantage of the latter is that the state variables considered include both forces and displacements. In this formulation, an optimization problem is solved at each time step to calculate the internal forces in the elements. This formulation was first proposed for the transient analysis of skeletal structure including plastic behavior [17,18]. Later, it was extended for the analysis of progressive collapse [19], thermoelectricity [20] and for base isolated structures [21].

A one dimensional (1-D) gap element has been developed and added in order to consider contact behavior [22]. The behavior of this element does not depend explicitly on the relative displacement between the two surfaces of the contact. This element is an additional function to the Lagrangian which describes the conservative components in the structural system. It has been shown that large time increments can be used and yet to maintain the convergence of the model.

In this paper, MLF is used to develop a numerical model for the analysis of SC-CBFs including multiple rocking joints. The gap element mentioned earlier is used to model the contact behavior at the rocking sections. In this model, the interaction between rocking sections sharing the same cable is considered automatically. The proposed model is used for the analysis of fifteen-story buildings, both with a traditional base rocking section and a building with multiple rocking sections. The proposed model showed a good convergence even when large time increments were used. This led to a relatively small computation time. In addition, it is shown that the flexural moments can be reduced significantly by applying the multiple rocking solution with a negligible effect on the displacements.

2. Numerical model for SC-CBF

2.1 General

A new model is developed for the analysis of SC-CBFs with multiple rocking joints based on MLF. MLF starts with the formulation of the Lagrangian and dissipation function of the dynamic system [18]. These functions describe the conservative and nonconservative characteristics of the system, respectively. The state variables in this formulation include a mixed description of forces and displacements in the dynamical system.

In the case where energy dissipation and contact exist, the Lagrangian and dissipation functions take the following [22]:

$$L\left(\mathbf{u},\mathbf{J},\dot{\mathbf{u}},\dot{\mathbf{J}}\right)=\frac{1}{2}\dot{\mathbf{u}}^{T}\mathbf{M}\dot{\mathbf{u}}+\frac{1}{2}\dot{\mathbf{J}}^{T}\mathbf{A}\dot{\mathbf{J}}+\mathbf{J}^{T}\mathbf{B}^{T}\dot{\mathbf{u}}+\mathbf{P}^{T}\mathbf{u}+g\left(\dot{\mathbf{J}}\right) \tag{1}$$

$$\bar{\varphi}\left(\dot{\mathbf{u}},\dot{\mathbf{J}}\right)=\frac{1}{2}\dot{\mathbf{u}}^{T}\mathbf{C}\dot{\mathbf{u}}+\varphi\left(\dot{\mathbf{J}}\right) \tag{2}$$

where **M** is the mass matrix in the global degrees of freedom (DOFs); **A** is the flexibility matrix in the local DOFs; **B** is equilibrium matrix that transfers the forces from the local DOFs to the global DOFs; **C** is damping matrix in the global DOFs; **u** is a vector of displacements in the global DOFs; **J** is a vector of impulses (time integral of forces) in the local DOFs; **P** is a vector of known external time dependent forces in the global DOFs; $\varphi(\dot{\mathbf{J}})$ is a function describes the potential of the dissipative elements as shown in Fig.1-a for elastic perfectly plastic material; $g(\dot{\mathbf{J}})$ is a function describes the gap element in the system as shown in Fig.1-b and upper dot represent time derivative.

The equations of motion and compatibility can be obtained when substituting the Lagrangian and the dissipation function into the Euler-Lagrange equations:

$$\frac{\mathrm{d}}{\mathrm{d}t}\left(\frac{\partial L}{\partial \dot{\mathbf{u}}}\right)-\left(\frac{\partial L}{\partial \mathbf{u}}\right)+\left(\frac{\partial \bar{\varphi}}{\partial \dot{\mathbf{u}}}\right)=\mathbf{0} \quad \rightarrow \quad \mathbf{M}\ddot{\mathbf{u}}+\mathbf{C}\dot{\mathbf{u}}+\mathbf{B}\dot{\mathbf{J}}=\mathbf{P} \tag{3}$$

$$\frac{\mathrm{d}}{\mathrm{d}t}\left(\frac{\partial L}{\partial \dot{\mathbf{J}}}\right)-\left(\frac{\partial L}{\partial \mathbf{J}}\right)+\left(\frac{\partial \bar{\varphi}}{\partial \dot{\mathbf{J}}}\right)=\mathbf{0} \quad \rightarrow \quad \mathbf{A}\ddot{\mathbf{J}}+\frac{\mathrm{d}}{\mathrm{d}t}\left(\frac{\partial g\left(\dot{\mathbf{J}}\right)}{\partial \dot{\mathbf{J}}}\right)+\frac{\partial \bar{\varphi}\left(\dot{\mathbf{J}}\right)}{\partial \dot{\mathbf{J}}}-\mathbf{B}^{T}\dot{\mathbf{u}}=\mathbf{0} \tag{4}$$

where Eqs. 3 and 4 represent the dynamic equilibrium and the compatibility of the velocities of the system, respectively. It has been shown [18] that these equations hold also when geometric nonlinearity is considered. Therefore, the proposed model can be easily extended to include geometrically nonlinear effects. However, this is beyond the scope of the current paper.

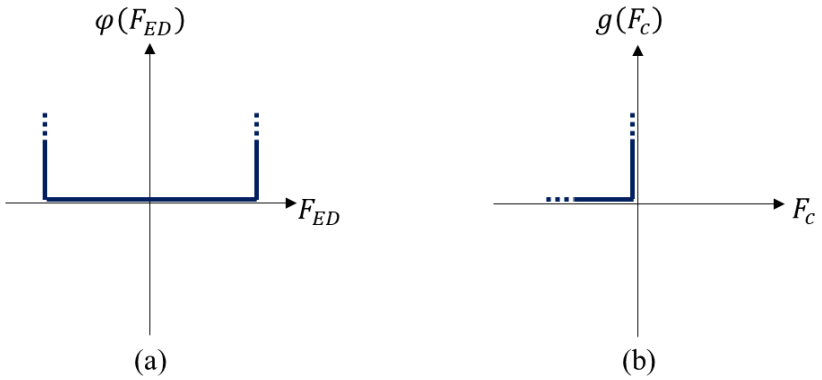

Fig.1 – Dissipation and gap functions in MLF: (a) 1-D dissipation function for elastic perfectly plastic material and (b) 1-D gap function for compression only element.

2.2 Implementing MLF for SC-CBF

In this paper, the MLF is adopted to develop a numerical scheme for the dynamic analysis of SC-CBFs with multiple rocking sections as shown schematically in Fig.2. The global DOFs represent the nodal displacements in the system. Each node includes two degrees of freedom representing the horizontal and the vertical displacements of each node. The local DOFs represent the internal forces in the structural elements at their local DOFs. The proposed model includes representation of the truss elements, ED elements, and cable elements. 1-D gap elements [22] are used to describe the column uplift at the rocking sections.

It is assumed that the energy dissipation in this system is concentrated at the rocking sections. Therefore, the truss elements are assumed to remain in their elastic region. Thus, these elements are modeled as 1-D elastic truss elements. Plastic behavior for the truss elements can be easily included by adding slider elements in series with the truss elements. Metallic yield dampers are added at each section, these elements are modeled using slider elements describing the plastic behavior in series with elastic springs describing the behavior of the ED elements in their elastic region as shown in Fig.2. The PT cables are modeled similarly to the truss elements. The force due to pre-stressing in these cables is added to the internal forces in the first time-step. The gap is assumed to be rigid in compression, and its behavior is described as shown in the previous section for 1-D gap element. Rigid link elements are added to prevent shear slide at the story levels. These elements are added as truss bars with large stiffness connecting horizontally the columns at the rocking levels.

The vector of internal forces includes the forces in the elements described above in their local DOFs and it is collected as follows: $\mathbf{F}=\{\mathbf{F}_T,\mathbf{F}_N,\mathbf{F}_C,\mathbf{F}_{ED}\}^T$; where $\mathbf{F}_T$, $\mathbf{F}_N$, $\mathbf{F}_C$ and $\mathbf{F}_{ED}$ are vectors of internal forces in the truss, cable, gap and ED elements, respectively. It is noted the shear link elements, in this case, are

included with the truss elements. These elements can be replaced using constraints; however, these methods are not in the scope of this paper.

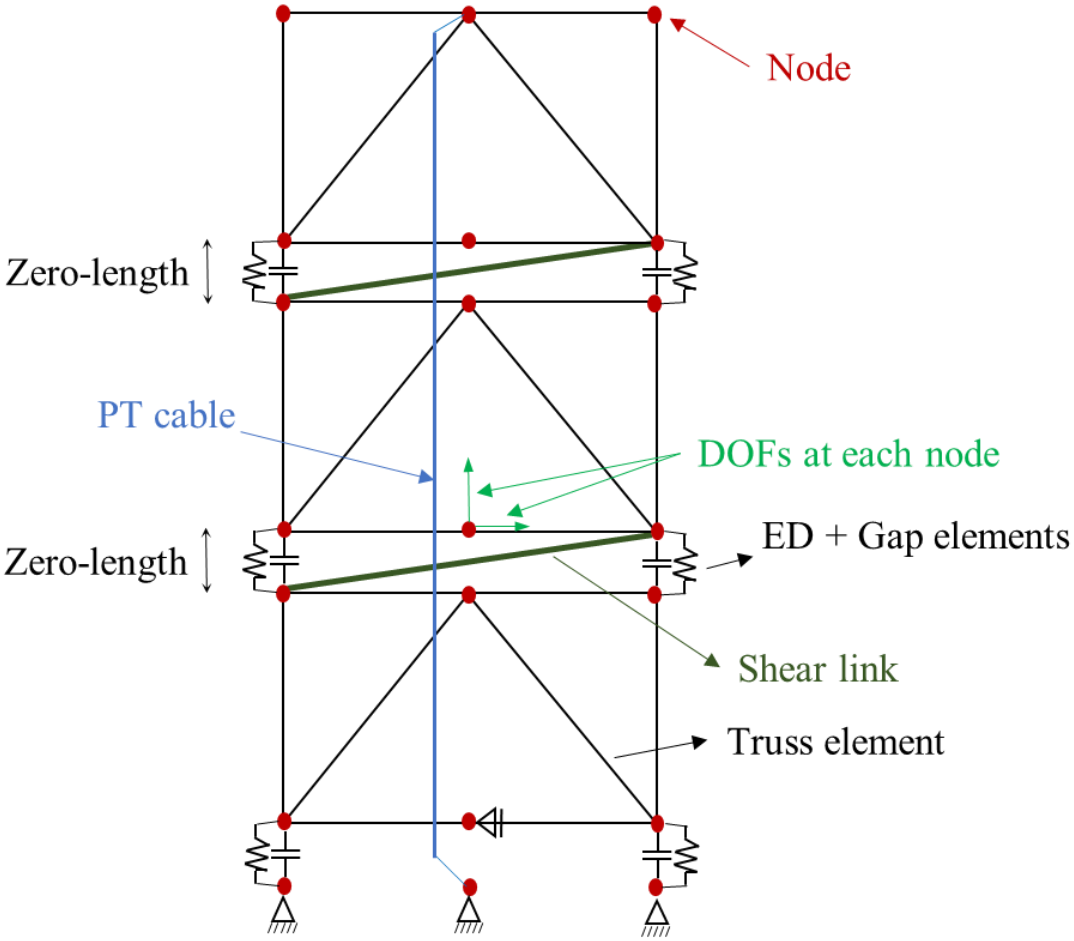

Fig.2 – Schematic representation of the proposed model and internal forces.

The equilibrium matrix includes the transformations of the internal forces of each type of element to the global degrees of freedom. These transformations include equilibrium equations and geometrical transformations. The general equilibrium matrix **B** is collected to include the structural elements as follows: $\mathbf{B} = \{\mathbf{B}_T, \mathbf{B}_N, \mathbf{B}_C, \mathbf{B}_{ED}\}^T$; where $\mathbf{B}_T$ is a matrix that transforms the internal forces in the truss elements shown in Fig.2 to the global DOFs; $\mathbf{B}_N$ transforms the internal force in the cable elements to the global DOFs, and it should be noted that several cables can be included in this formulation with different configurations; $\mathbf{B}_C$ is a matrix that transforms the internal forces in the gap element to the rocking surface and $\mathbf{B}_{ED}$ is a matrix that transforms the internal forces in the ED elements to the rocking sections.

2.3 Time discretization

Eqs. 3 and 4 are discretized in time using the mid-point rule central differences. It has been shown that the latter leads to momentum conservation [17]. The discretized equations take the following after replacing $\dot{\mathbf{u}}$ with **v** and $\dot{\mathbf{J}}$ with **F**:

$$\mathbf{M}\left(\frac{\mathbf{v}_{n+1}-\mathbf{v}_n}{\Delta t}\right)+\mathbf{C}\left(\frac{\mathbf{v}_{n+1}+\mathbf{v}_n}{2}\right)+\mathbf{B}\left(\frac{\mathbf{F}_{n+1}+\mathbf{F}_n}{2}\right)=\left(\frac{\mathbf{P}_{n+1}+\mathbf{P}_n}{2}\right) \quad (5)$$

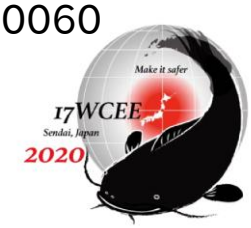

$$\mathbf{A}\left(\frac{\mathbf{F}_{n+1}-\mathbf{F}_n}{\Delta t}\right)+\frac{1}{2}\left(\left.\frac{\partial\varphi(\mathbf{F})}{\partial\mathbf{F}}\right|_{n+1}+\left.\frac{\partial\varphi(\mathbf{F})}{\partial\mathbf{F}}\right|_{n}\right)+\frac{1}{\Delta t}\left(\left.\frac{\partial g(\mathbf{F})}{\partial\mathbf{F}}\right|_{n+1}-\left.\frac{\partial g(\mathbf{F})}{\partial\mathbf{F}}\right|_{n}\right)-\mathbf{B}^T\left(\frac{\mathbf{v}_{n+1}-\mathbf{v}_n}{\Delta t}\right)=\mathbf{0} \quad (6)$$

In the proposed model, several DOFs do not include mass. This leads to a singular mass matrix. Eliminating the velocity vector $\mathbf{v}_{M,n+1}$ where the subscript M represents the DOFs including mass gives:

$$\mathbf{v}_{M,n+1}=\mathbf{M}_1\left[\mathbf{M}_2\mathbf{v}_{M,n}-\mathbf{B}_M\left(\frac{\mathbf{F}_{n+1}+\mathbf{F}_n}{2}\right)+\left(\frac{\mathbf{P}_{n+1}+\mathbf{P}_n}{2}\right)\right] \quad (7)$$

where;

$$\mathbf{M}_1=\left(\frac{\bar{\mathbf{M}}}{\Delta t}+\frac{\bar{\mathbf{C}}}{2}\right)^{-1},\quad \mathbf{M}_2=\left(\frac{\bar{\mathbf{M}}}{\Delta t}-\frac{\bar{\mathbf{C}}}{2}\right) \quad (8)$$

and,

$\bar{\mathbf{M}}$ is a diagonal matrix including the nodal masses at global DOFs for nodes with concentrated mass; $\bar{\mathbf{C}}$ is the damping matrix; $\mathbf{B}_M$ is a matrix including the M-th columns of the general equilibrium matrix $\mathbf{B}$ and Δt is the time increment in seconds.

The compatibility equation takes the following after discretization substituting $\mathbf{v}_{M,n+1}$:

$$\bar{\mathbf{A}}\mathbf{F}_{n+1}+\frac{1}{2}\left.\frac{\partial\varphi(\mathbf{F})}{\partial\mathbf{F}}\right|_{n+1}+\frac{1}{\Delta t}\left.\frac{\partial g(\mathbf{F})}{\partial\mathbf{F}}\right|_{n+1}+\bar{\mathbf{b}}-\frac{1}{2}\mathbf{B}_S^T\mathbf{v}_{S,n+1}-\frac{1}{2}\mathbf{B}_F^T\mathbf{v}_{F,n+1}=\mathbf{0} \quad (9)$$

where;

$$\bar{\mathbf{A}}=\frac{\mathbf{A}}{\Delta t}+\frac{1}{4}\mathbf{B}_M^T\mathbf{M}_1\mathbf{B}_M \quad (10)$$

and,

$$\bar{\mathbf{b}}=\left\{\left(-\frac{\mathbf{A}}{\Delta t}+\frac{\mathbf{B}_M^T}{2}\mathbf{M}_1\frac{\mathbf{B}_M}{2}\right)\mathbf{F}_n-\frac{1}{\Delta t}\left.\frac{\partial g(\mathbf{F})}{\partial\mathbf{F}}\right|_n+\frac{1}{2}\left.\frac{\partial\varphi(\mathbf{F})}{\partial\mathbf{F}}\right|_n\right.$$
$$\left.-\left(\frac{\mathbf{B}_M^T}{2}+\frac{\mathbf{B}_M^T}{2}\mathbf{M}_1\mathbf{M}_2\right)\mathbf{v}_{M,n}-\frac{\mathbf{B}_M^T}{2}\mathbf{M}_1\left(\frac{\mathbf{P}_{n+1}+\mathbf{P}_n}{2}\right)\right\} \quad (11)$$

The initial prestress force is added as the value of $\mathbf{F}_N$ at the first time-step. This is used to calculate the initial value of the vector $\bar{\mathbf{b}}$.

2.4 Time step solution

The vector that includes the velocities of the system at the global DOFs $\mathbf{v}$ (Eq. 7) is dependent explicitly on the internal forces $\mathbf{F}$. Therefore, the main equation to be solved at each time increment is the compatibility equation (Eq. 9). In this equation, the matrix $\bar{\mathbf{A}}$ is positive semi-definite since it is obtained by summing positive matrices. Hence, it can be easily shown that this equation is the first optimality criteria of the following optimization problem:

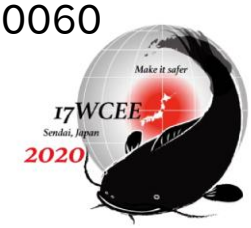

$$
\begin{aligned}
&\min \ \frac{1}{2}\mathbf{F}_{n+1}^{T}\bar{\mathbf{A}}\mathbf{F}_{n+1}+\bar{\mathbf{b}}^{T}\mathbf{F}_{n+1}\\
&\text{s.t}\\
&\frac{1}{2}\varphi\left(\mathbf{F}_{n+1}\right)\le 0\\
&\frac{1}{\Delta t}g\left(\mathbf{F}_{n+1}\right)\le 0\\
&\mathbf{B}_{S}\mathbf{F}_{S,n+1}=\mathbf{F}_{S,external}\\
&\mathbf{B}_{F}\mathbf{F}_{F,n+1}=\mathbf{0}
\end{aligned}
\tag{12}
$$

The optimization problem in Eq. 12 includes the internal forces in the structural elements as design variables. The constraints of the optimization problem include the ED and gap elements. In addition, equilibrium at the degrees of freedom where dynamic forces do not present is received as equality constraints of the optimization problem. This optimization problem can be solved easily using available nonlinear optimization solvers such as *fmincon* in MATLAB [23].

2.5 Solution scheme

The solution of the dynamic system starts with setting the initial conditions. The forces due to the pre-stress of the cable elements are substituted in the force vector **F**. Later, the matrix $\bar{\mathbf{A}}$ and the vector $\bar{\mathbf{b}}$ are calculated from the structural data. At this stage, an incremental solution starts with computing the internal forces in the structural elements by solving the optimization problem described in Eq. 12 for each time step.

Table 1 – MLF Computational Procedure

step	Calculation
Step 1	Calculate the initial vector of internal forces at t=0
Step 2	Calculate the matrix $\bar{\mathbf{A}}$ and the vector $\bar{\mathbf{b}}$ from Eqs. 10 and 11
Step 3	Calculate $\frac{\partial\varphi}{\partial\mathbf{F}}\Big\vert_{n+1}$ and $\frac{\partial g}{\partial\mathbf{F}}\Big\vert_{n+1}$ by substituting the values of the vector $\mathbf{F}_{n+1}$ in the derivative of the dissipation and gap functions, respectively.
Step 4	Calculate the velocities in DOFs without dynamic forces using the Lagrange multipliers of the equality constraints of the optimization problem from Eq. 12.
Step 5	Solve Eq. 7 for calculating the velocities in DOFs with dynamic forces.
Step 6	Calculate the displacements and velocities at current time step using Eqs. 13 and 14 respectively.
Step 7	Return to step 2 for calculating the next time step.

With the vector of internal forces at hand, the vectors $\frac{\partial\varphi}{\partial\mathbf{F}}\Big\vert_{n+1}$ and $\frac{\partial g}{\partial\mathbf{F}}\Big\vert_{n+1}$ can be calculated by substituting the values of the vector **F** in the dissipation and gap functions and calculating the derivative. It has been shown that the velocities at DOFs without dynamic forces can be obtained from the Lagrange multipliers of the equality constraints [17]. The velocity at DOFs with dynamic forces can be calculated by solving Eq. 7. The displacements and accelerations can be calculated from the velocities as shown in Eqs. 13 and 14. For convenience, a pseudo-code of the numerical integration scheme is summarized in Table. 1.

$$\mathbf{u}_{n+1} = \mathbf{u}_n + \Delta t\left(\frac{\mathbf{v}_{n+1} + \mathbf{v}_n}{2}\right) \tag{13}$$

$$\ddot{\mathbf{u}}_{n+1} = \frac{\mathbf{v}_{n+1} - \mathbf{v}_n}{\Delta t} \tag{14}$$

3. Case Study

A fifteen-story building with a lateral load resisting system of SC-CBFs was modeled using the proposed procedure. The plan of the building is shown in Fig.3. The wall was modeled using the planar model described in previous sections as shown in Fig.2. The building was subjected to the ground acceleration LA07 in the horizontal direction. The story mass was 1000 [ton] and it is constant with the building height. It is assumed that this mass distributes equally between the four SC-CBFs in the horizontal direction. Therefore, the analyzed SC-CBF had a story mass of 250 [ton] at each story level.

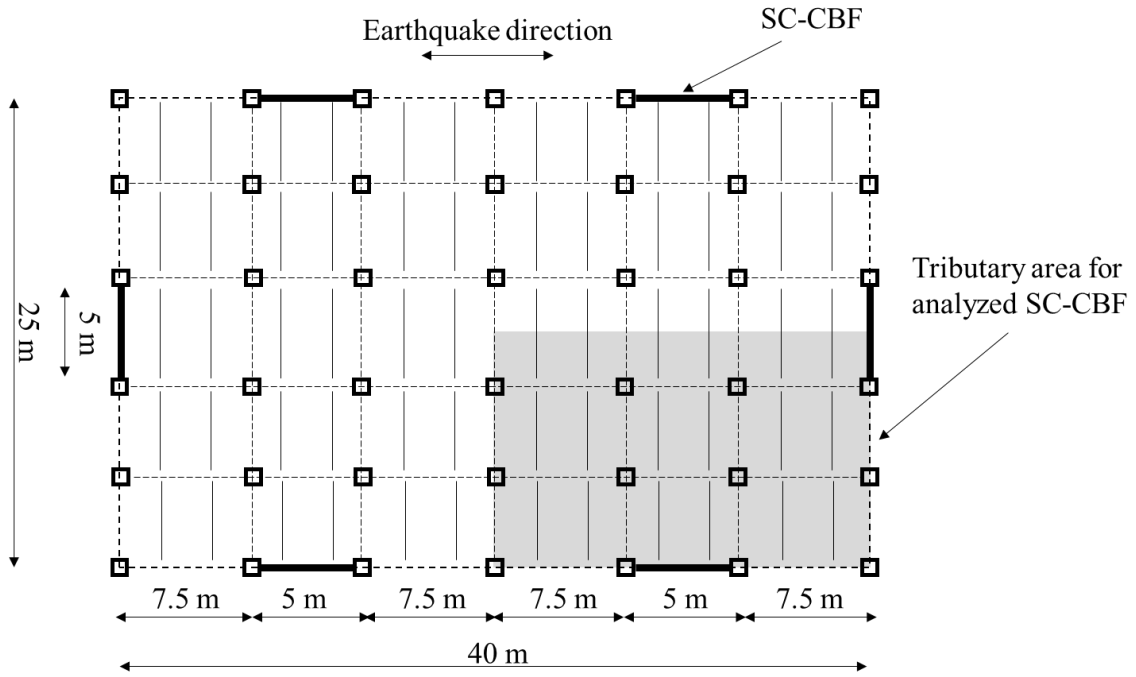

Fig.3 – Floor plan of 15 story building with SC-CBFs.

Two models were built; in the first model, the rocking section was designed only at the base of the building. Additional rocking sections through the wall height were designed in the second building at the base of stories 5, 9 and 13. A single cable was connected to the top of the building and anchored to the foundation in both examples. The initial pre-stress was 50% of the ultimate stress of the PT cable material which has an ultimate strength of 1860 $[MPa]$. Metallic yield dampers with a sectional area of 8 $[cm^2]$ and yield stress of 400 $[MPa]$ were provided at each rocking section at the edges of the rocking sections. Initial stiffness proportional Rayleigh damping of 5% was assigned to the first and seconds vibration modes.

The truss elements were designed to remain elastic during the seismic action. The yield was concentrated only at the ED material. The sectional area of the diagonal elements was 90 $[cm^2]$ and it was constant through the building height. Similarly, the columns sectional area was constant through the wall height and it was 130 $[cm^2]$.

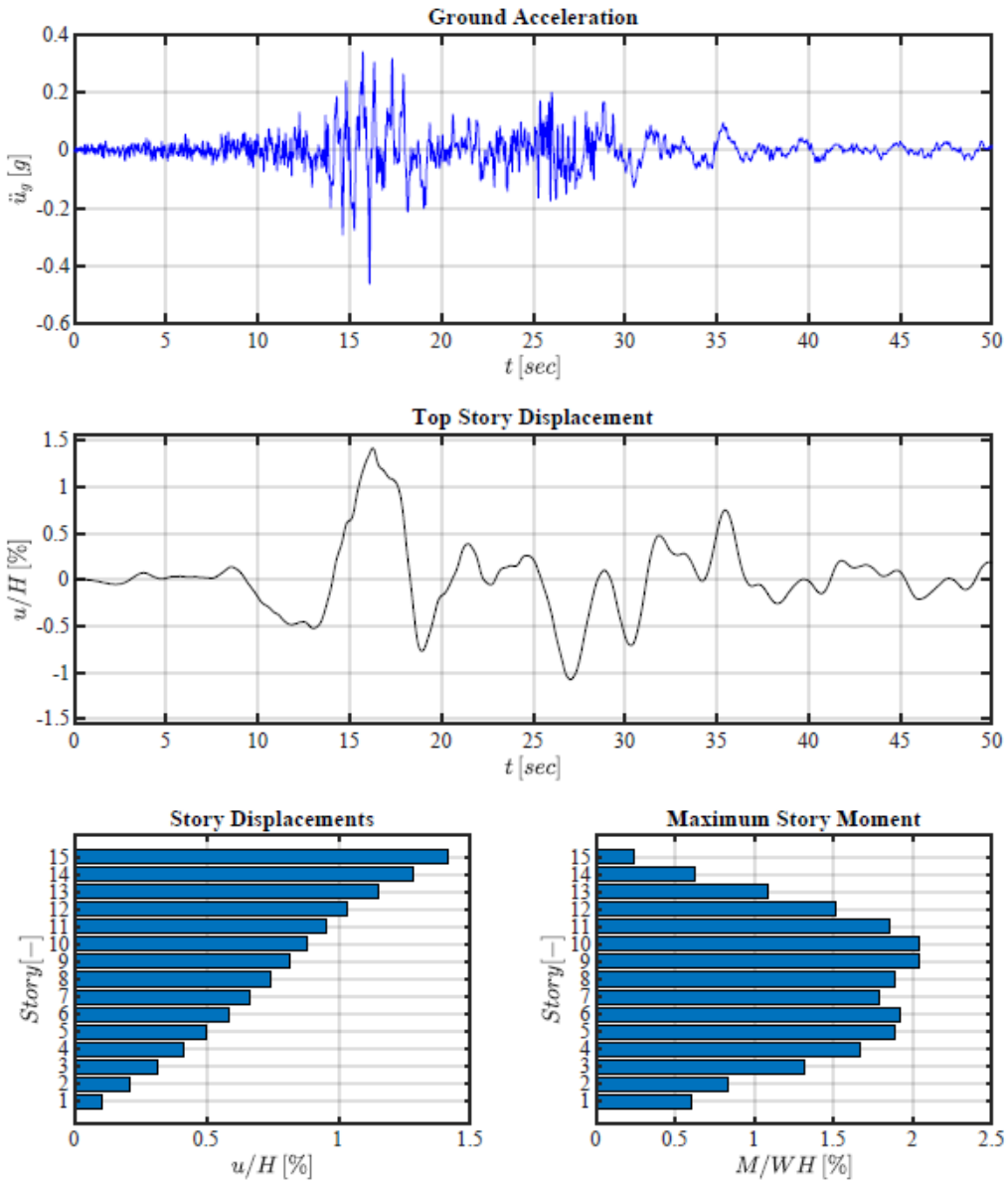

Fig.4 – Structural response of SC-CBF with base rocking: the top plot shows the LA07 ground acceleration, the middle plot shows the displacement of the top story, the left-bottom plot shows the maximum displacements at each story level and the right-bottom plot shows the maximum moment at each story level.

The analyses of both buildings were conducted using the proposed model with a constant time step size of 0.02 [sec]. This time increment was chosen based on the data of the ground acceleration. The analysis with smaller time step size did not affect the results; however, this validation is not presented herein due to space limitations. Fig.4 shows the results obtained for the case of base rocking SC-CBF. The ground acceleration is shown at the top plot of the figure and the displacement of the top story is shown in the middle plot. The maximum displacement at the top story was less than 1.5% of the building height. This displacement was the largest through the building height. In the left bottom plot of Fig.4, the maximum story displacements are presented. It is shown the displacement profile is approximately linear. This result was expected since the plastic rotations were designed only at the base of the building. The maximum flexural moments are shown in the right bottom plot of Fig.4. The higher vibration mode effects can be easily observed. The largest flexural

moment, in this case, was approximately 3 times larger than the moment at the rocking section and it was in the 9-th story.

In the second example, multiple rocking sections were designed. The rocking sections at higher levels were designed at the base of stories 5, 9 and 13 in addition to the base rocking section. As expected, these additional rocking sections decreased significantly the flexural moments as shown in Fig.5. This caused a reduction in the internal forces in the truss elements. This reduction may reduce significantly the cost of the building. Moreover, only a negligible increase in the story displacements was observed. These results are in agreement with other studies on rocking walls or SC-CBFs with multiple rocking sections [12,13].

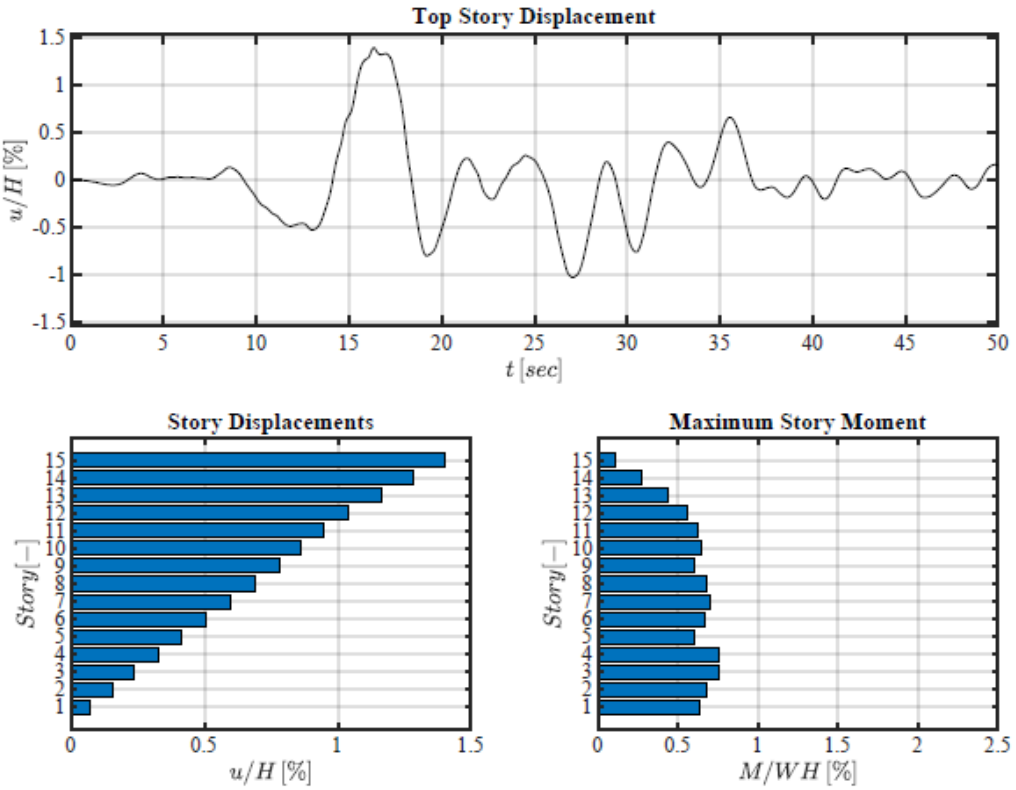

Fig.5 – Structural response of SC-CBF with multiple rocking sections: the top plot shows the displacement of the top story, the left-bottom plot shows the maximum displacements at each story level and the right-bottom plot shows the maximum moment at each story level.

5. Conclusions

In this paper, a new model for the analysis of SC-CBFs with multiple rocking sections was developed. This model is based on the MLF in which the state variables include the displacements and the forces in the dynamic system. The contact behavior was described using 1-D gap elements which do not depend explicitly on the relative displacement between the adjacent surfaces of the rocking section.

An example of fifteen-story building was presented, the results show that the behavior of such systems can be easily obtained using the proposed procedure. In MLF momentum conservation is automatically considered, therefore, convergence issues due to contact behavior at the rocking section are prevented.

Large time increments were used for the analysis when using the proposed model. Therefore, the calculation time is small. This is very important when excessive number of analysis is needed, such as in life cycle cost analysis or for building surrogate models.

The presented formulation is robust, and it can be easily extended for the analysis of asymmetrical three-dimensional buildings.

6. References

[1] Chung, R.M. (1996) The January 17, 1995 Hyogo-ken-Nanbu (Kobe) Earthquake: performance of structures, lifelines, and fire protection systems. US Department of Commerce, Technology Administration, National Institute of Standards and Technology.

[2] Kajitani, Y., Chang, S.E. and Tatano, H. (2013) Economic Impacts of the 2011 Tohoku-oki earthquake and tsunami. *Earthquake Spectra*, **29**, 457–78. https://doi.org/10.1193/1.4000108

[3] Potter, S.H., Becker, J.S., Johnston, D.M. and Rossiter, K.P. (2015) An overview of the impacts of the 2010-2011 Canterbury earthquakes. *International Journal of Disaster Risk Reduction*, Elsevier. **14**, 6–14. https://doi.org/10.1016/j.ijdrr.2015.01.014

[4] Nakashima, M., Lavan, O., Kurata, M. and Luo, Y. (2014) Earthquake engineering research needs in light of lessons learned from the 2011 Tohoku earthquake. *Earthquake Engineering and Engineering Vibration*, **13**, 141–9. https://doi.org/10.1007/s11803-014-0244-y

[5] Christopoulos, C., Pampanin, S. and Nigel Priestley, M.J. (2003) Performance-based seismic response of frame structures including residual deformations. Part I: Single-Degree of Freedom Systems. *Journal of Earthquake Engineering*, **7**, 97–118. https://doi.org/10.1080/13632460309350444

[6] Tremblay, R., Poirier, L., Bouaanani, N., Leclerc, M., Rene, V., Fronteddu, L. et al. (2008) Innovative Viscously Damped Rocking Braced Steel Frames. *The 14th World Conference on Earthquake Engineering (14 WCEE), October 12-17,*.

[7] Deierlein, G.G., Ma, X., Eatherton, M., Krawinkler, H., Billington, S. and Hajjar, J. (2009) Collaborative Research on Development of Innovative Steel Braced Frame Systems with Controlled Rocking and Replaceable Fuses. *In Proc 6th International Conference on Urban Earthquake Engineering, Tokyo*, 413–6.

[8] Chancellor, N., Eatherton, M., Roke, D. and Akbaş, T. (2018) Self-Centering Seismic Lateral Force Resisting Systems: High Performance Structures for the City of Tomorrow. *Buildings*, **4**, 520–48. https://doi.org/10.3390/buildings4030520

[9] Roke, D., Sause, R., Ricles, J.M., Seo, C.-Y. and Lee, K.-S. (2006) Self-Centering Seismic-Resistant Steel Concentrically-Braced Frames. *Proceedings of the 8th US National Conference on Earthquake Engineering, EERI, San Francisco, April*, 18–22.

[10] Midorikawa, M., Azuhata, T., Ishihara, T. and Wada, A. (2006) Shaking table tests on seismic response of steel braced frames with column uplift. *Earthquake Engineering and Structural Dynamics*, 1767–85. https://doi.org/10.1002/eqe

[11] Eatherton, M., Hajjar, J., Deierlein, G., Ma, X. and Krawinkler, H. (2010) Hybrid Simulation Testing of a Controlled Rocking Steel Braced Frame System. *Proceedings of the 9th US National and 10th Canadian Conference on Earthquake Engineering*, Toronto, Ontario, Canada.

[12] Wiebe, L. and Christopoulos, C. (2009) Mitigation of Higher Mode Effects in Base-Rocking Systems by Using Multiple Rocking Sections. *Journal of Earthquake Engineering*, Taylor & Francis Group. **13**, 83–108. https://doi.org/10.1080/13632460902813315

[13] Li, T., Berman, J.W. and Wiebe, R. (2017) Parametric study of seismic performance of structures with multiple rocking joints. *Engineering Structures*, Elsevier Ltd. **146**, 75–92. https://doi.org/10.1016/j.engstruct.2017.05.030

[14] Dyanati, M., Huang, Q. and Roke, D. (2017) Cost-benefit evaluation of self-centring concentrically braced frames considering uncertainties. *Structure and Infrastructure Engineering*, Taylor & Francis. **13**, 537–53.

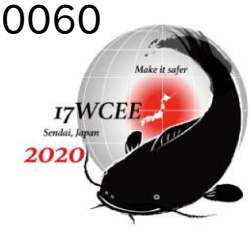

https://doi.org/10.1080/15732479.2016.1173070

[15] Sause, R., Ricles, J.M., Roke, D.A., Chancellor, N.B. and Gonner, N.P. (2010) Seismic performance of a self-centering rocking concentrically-braced frame. *Proceedings of the 9th US National and 10th Canadian Conference on Earthquake Engineering*, 25–9.

[16] Carpenter, N.J., Taylor, R.L. and Katona, M.G. (1991) Lagrange constraints for transient finite element surface contact. *International Journal for Numerical Methods in Engineering*, **32**, 103–28. https://doi.org/10.1002/nme.1620320107

[17] Sivaselvan, M. V and Reinhorn, A.M. (2004) Nonlinear Structural Analysis Towards Collapse Simulation: A Dynamical System Approach. *Technical Report MCEER-04-0005*,. https://doi.org/10.1016/j.jse.2005.10.002

[18] Sivaselvan, M. V. and Reinhorn, A.M. (2006) Lagrangian Approach to Structural Collapse Simulation. *Journal of Engineering Mechanics*, **132**, 795–805. https://doi.org/10.1061/(ASCE)0733-9399(2006)132:8(795)

[19] Lavan, O., Sivaselvan, M. V., Reinhorn, A.M. and Dargush, G.F. (2009) Progressive collapse analysis through strength degradation and fracture in the Mixed Lagrangian Formulation. *Earthquake Engineering and Structural Dynamics*, 1483–504. https://doi.org/10.1002/eqe

[20] Apostolakis, G. and Dargush, G.F. (2012) Mixed Lagrangian Formulation for Linear Thermoelastic Response of Structures. *Journal of Engineering Mechanics*, **138**, 508–18. https://doi.org/10.1061/(ASCE)EM.1943-7889.0000346

[21] Oliveto, N.D. and Athanasiou, A. (2019) 2D dynamic and earthquake response analysis of base isolation systems using a convex optimization framework. *Annals of Solid and Structural Mechanics*, Springer Berlin Heidelberg. **11**, 11–24. https://doi.org/10.1007/s12356-019-00053-4

[22] Lavan, O. (2010) Dynamic analysis of gap closing and contact in the mixed lagrangian framework: Toward progressive collapse prediction. *Journal of Engineering Mechanics*, **136**, 979–86. https://doi.org/10.1061/(ASCE)EM.1943-7889.0000146

[23] The MathWorks Inc. (2016) Matlab. The MathWorks, Inc.

